Materials Science-Poland, 42(1), 2024, pp. 92-106
http://www.materialsscience.pwr.wroc.pl/
DOI: 10.2478/msp-2024-0008

Analysis of the influence of dies geometry on the process extrusion force and properties of the extrudate obtained in the process of cold extrusion of 7075 aluminum alloy by the KOBO method

Marek Zwolak*, Romana Śliwa

Department of Materials Forming and Processing, The Faculty of Mechanical Engineering and Aeronautics, Rzeszów University of Technology

The KOBO extrusion process is an unconventional method of extrusion based on the phenomenon of superplasticity as an effect of a special state caused by the oscillatory motion of the die at a certain angle a certain frequency. It significantly lowers the extrusion force and makes it possible to extrude lightweight metals and alloys (e.g. aluminum and magnesium alloys) in cold extrusion with high extrusion ratios compared to conventional hot extrusion.
This work studies the influence of the tool (die) geometry on process realization parameters and the properties of the extrudate. Experimental studies of cold KOBO extrusion were performed using dies with different face portion geometry. The obtained extrudate obtained from EN-AW 7075 aluminum billets was examined for mechanical properties and macro/microstructure, showing that, with adequate modifications to the tool face part geometry, it is possible to lower the extrusion force and obtain extrudate with desired properties.

Keywords: *aluminum extrusion, KOBO method, 7075 aluminum, bulk forming*

1. Introduction

The KOBO method [1, 2] is an unconventional bulk material forming method based on cyclic change of the deformation path and localized plastic flow of material [3]. In most cases, the KOBO method is applied in the form of a direct extrusion, where the change of deformation path is realized by cyclic oscillation of the die, with given frequency and at a given angle (Fig. 1).

The most significant advantage of the KOBO extrusion is that it enables the cold extrusion (without preheating the billet and press/tooling parts) with a high extrusion ratio (on the order of several hundred [4]) of nonferrous metals and alloys, even those considered hard to extrude (e.g. EN-AW 7075 aluminum alloy). These properties of the KOBO method are associated with the concentration of lattice defects (Frenkel defects) in the billet zone closest to the die face, which is subjected to cyclic, high deformation in complex strain conditions. This leads to fluid-like flow of extruded material [5, 6] with radial plastic flow scheme [7].

The KOBO extrusion method, besides being an effective method of grain refinement in extruded material [8], gives an opportunity to model the effect of process parameters, such as die oscillation frequency and extrusion speed, on the extrudate's microstructure and mechanical properties [9]. These parameters may also be changed during the process (constant force extrusion). By changing those parameters, it is possible to significantly lower extrusion force as well [10].

Constitutive models of the extrusion of commercially pure lead with cyclic torsion (not the KOBO method *per se*) showed that cyclic torsion leads to material softening and significantly lowers extrusion force [11, 12]. Upper-bound analysis of KOBO extrusion [13] showed that die oscillation during extrusion forms a radial plastic flow zone

* E-mail: m.zwolak@prz.edu.pl

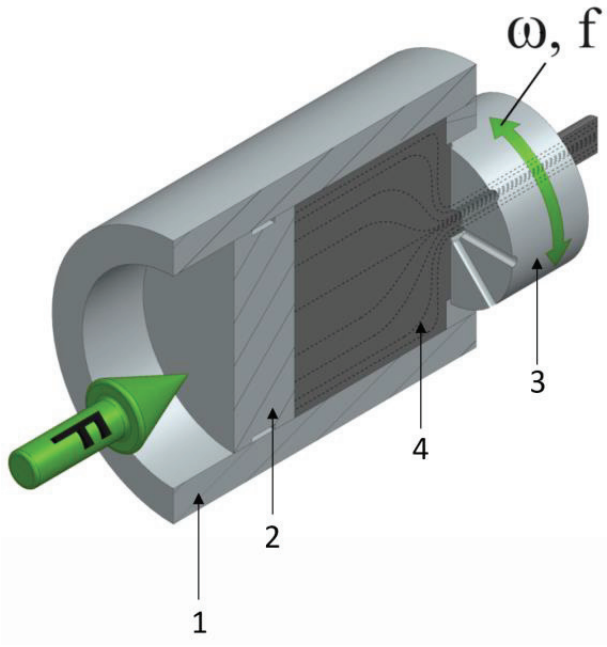

Fig. 1. Schematic of KOBO extrusion process: 1- container sleeve, 2- butt, 3- die, 4- billet

near the die face surface in which extruded material undergoes high accumulated plastic deformation; this mechanism lowers extrusion force. This analysis was compared to the experimental data and was proven to be convergent in steady state extrusion.

The attempts to model the KOBO method with FEM methods that have been presented in a few publications [14, 15] are based on specific cases, simplified models and a very narrow range of process parameters. No numerical model of KOBO extrusion has been validated through experimentation, especially considering both mechanical and thermal aspects of the process as well as tooling geometry.

The tooling for KOBO extrusion differs from that used in conventional extrusion. The front portion of the oscillating die has a direct effect on the introduction of complex strain conditions in the extruded billet, yet the geometry of the dies' front surface is mostly neglected in experimental work. Therefore, this work is focused on the impact of die geometry on the KOBO extrusion process. Based on preliminary research [7], the most favorable geometry of the front portion of the die was chosen. The experimental research presented in this paper shows the effect of die face geometry modification on extrusion force and the obtained extrudate's structure and mechanical properties.

2. Experimental procedure

Extrusion tests were carried out on a direct extrusion KOBO press (Fig. 2) with characteristic parameters: maximum extrusion force of 2500 kN and maximum torque on the die of 2606 Nm.

The material chosen for experimental research was commercially bought EN AW-7075 T6 aluminum alloy in the form of an extruded round bar 60 mm in diameter. The material was cut into pieces 60 mm in length and annealed in the following cycle: heating and stabilizing the temperature to 415°C, holding for 180 minutes, cooling at 10°C/h to below 200°C and finally air cooling to room temperature. Obtained billets have tensile strength of R_m∼205 MPa at ∼12% elongation (average from three control samples) and hardness ∼69 HV0.1 (average from three measurements). Aluminum alloy 7075 in the annealed state has a much lower tensile strength than in the T6 state but

Fig. 2. 2500 kN KOBO extrusion press

relatively low elongation at break in the uniaxial tensile test.

The effect of the annealing process on the internal structure of the material was grain growth in the axial direction (Fig. 3).

The microstructure of alloy 7075 in the initial state (reference sample) is typical of the alloy after the annealing process (Fig. 4) [16, 17]. It consists of a matrix, a solid solution of alloying elements in aluminum with fine separations of irregularly shaped $MgZn_2$ phase particles, large separations of $FeAl_3$ intermetallic phase particles and a dispersive strengthening phase of Mg_2Si (Fig. 4).

All tests were carried out with the same process parameters: extrusion speed 0.1 mm/s, die oscillation angle $\pm 8^\circ$, die oscillation frequency 7Hz, cold extrusion (without preheating billets and tooling), extrusion ratio λ=36.

For comparison, a conventional extrusion test with heating of the press container and ingot to 450°C was also performed.

Based on preliminary research [7], a die face geometry with radial grooves and a small prechamber was chosen (Fig. 5). In all cases, the bearing length was 3 mm. The only modification to the die face geometry was varying the number and depth of the grooves (Fig. 6, Table 1). The active diameter of the die was 44 mm (for a 60 mm billet). All dies were made of 1.2343 tool steel, hardened and tempered to ~56 HRC. A total of seven dies were used for experimental research, six with grooves and one with a flat face part for comparison. For easier identification of die geometry and corresponding results, each die geometry was given a code in the form GxDx: Gx represents the number of grooves, Dx represents the depth of the grooves, and NG indicates no grooves (Fig. 6). The tests were carried out in three series. Each series tested three different dies (one die per test). Adequate time elapsed between each test for press parts to cool down to room temperature.

Samples for tensile test and microscopic examination were prepared from front, middle and end sections of obtained extrudate (shortened to F, M, E later in text). Tensile tests were made according to the ISO 6892-1:2016 standard. Metallographic samples were prepared by mechanical grinding and polishing and etched with Kellers reagent according to the ASTM E407 standard. Macro

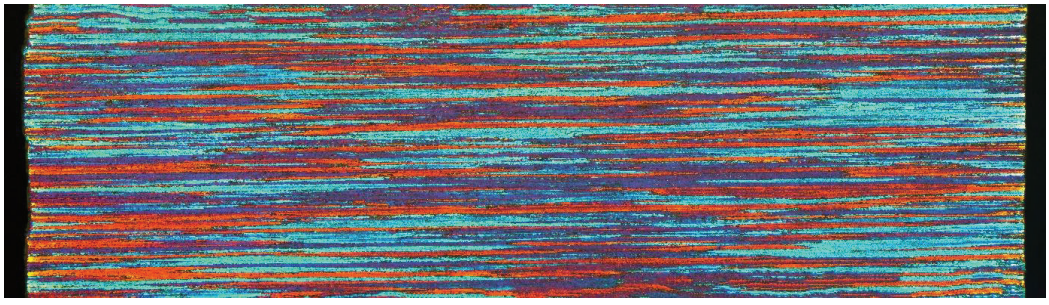

Fig. 3. Macrostructure of the longitudinal section of the test material in the initial state (annealed 7075 aluminum alloy)

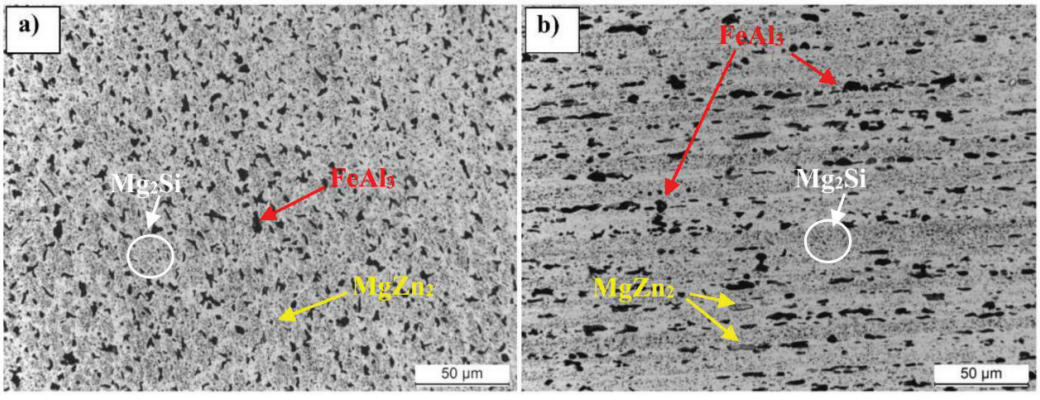

Fig. 4. Microstructures of 7075 aluminum alloy initial condition, cross-section (a) and longitudinal section (b), 500x mag

Table 1. Dimensions of the characteristic features of the dies used for experimental research

Code	Number of grooves	Grooves depth [mm]
G8D1	8	1
G8D2	8	2
G8D3	8	3
G6D1	6	1
G10D1	10	1
G12D1	12	1
NG	–	–

and microstructure examination were made with a metallographic microscope and SEM.

3. Results and discussion

The graph in Figure 7 records the extrusion forces as a function of stem displacement.

The first G8D1 test was disturbed by starting the extrusion process without first cleaning the container sleeve, which resulted in an increase in the resistance to pushing the butt through the container sleeve during the execution of the test. The force of pushing the butt during the cleaning of the press container sleeve is given in Table 2. After cleaning the sleeve, the force of pushing the butt was negligible.

The maximum value of the extrusion force varies depending on the die variant used (Fig. 7, Table 2). For the first three tests, excluding the first trial, the maximum extrusion force reached the same values regardless of the die variant used. For the next three tests (series 2), the maximum extrusion force decreases with the change in tool geometry: the minimum force, 1890 kN, was obtained for the test made with the die with the largest number (12) of grooves with the smallest depth (1 mm). For the conventional hot extrusion test, an extrusion force lower than in all cases of cold extrusion in the KOBO process was obtained. There is a noticeable

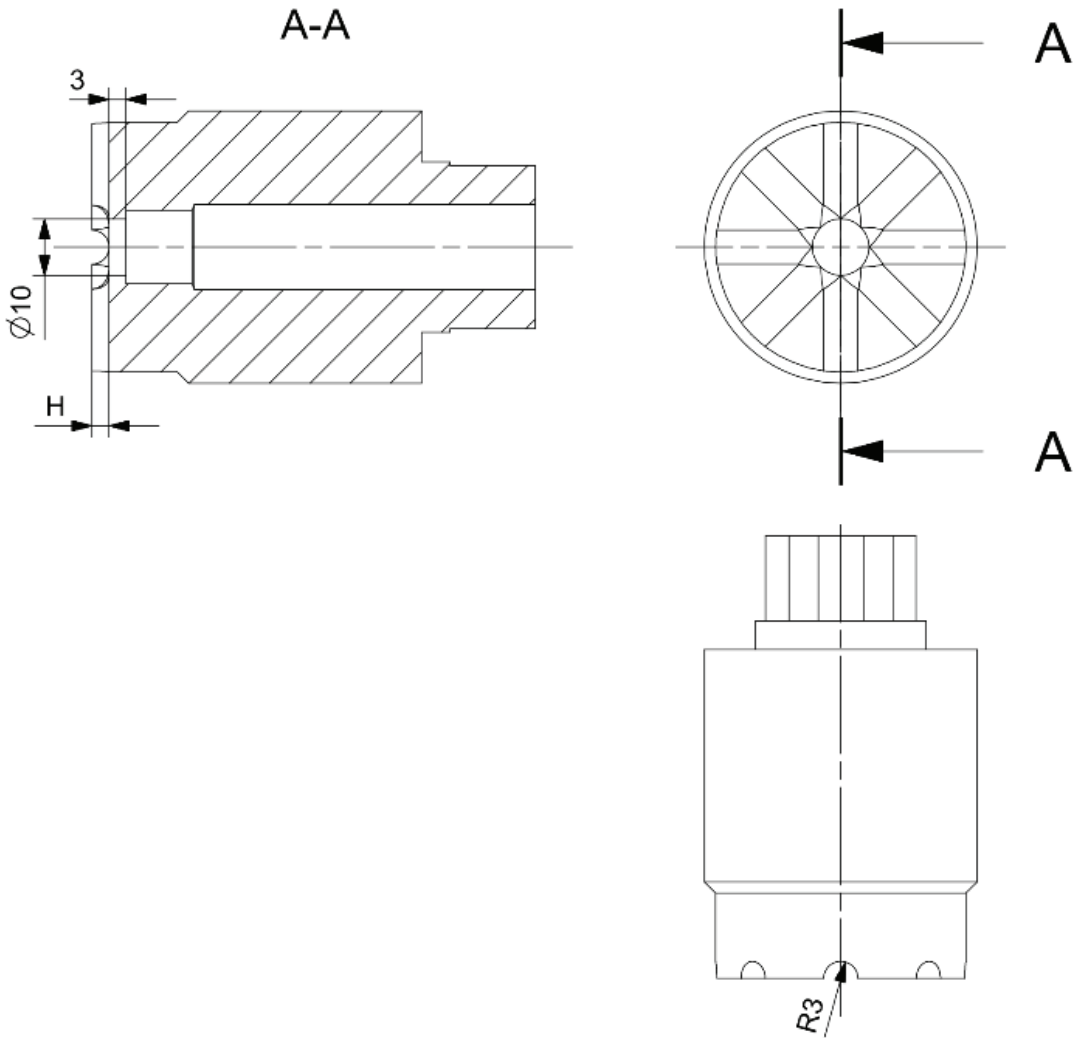

Fig. 5. Sketch of characteristic features of dies for KOBO process

increase in force at the final stage of extrusion, which is characteristic of the conventional process but does not occur in the case of KOBO extrusion. The maximum extrusion force of the press (2500 kN) was not reached for any of the cases.

A static tensile test was carried out in each of the three series, adequate for the course of the experimental study. The results of the first series of tests showed that the material underwent deformational strengthening. Regardless of the tool used, the tensile plots (Fig. 8) and the determined strength properties (Table 3) are comparable. In two cases, the test showed a slightly higher value of tensile strength; both cases were samples from the final part of the extrudate and were probably cooled slightly faster than the rest of the extrudate during the opening of the press container after the extrusion process. The difference is ∼20 MPa higher than the series average.

The results of the second series showed that the material underwent deformational strengthening adequately with the first series. Regardless of the tool used, the tensile plots (Fig. 9) and the determined strength properties (Table 4) are comparable. The yield strength value marked in red in Table 4 is the result of software error, the value is not correct.

The results of the third series of samples (Fig. 10, Table 5) showed that a die without grooves (NG KOBO) produced extrudate with strength

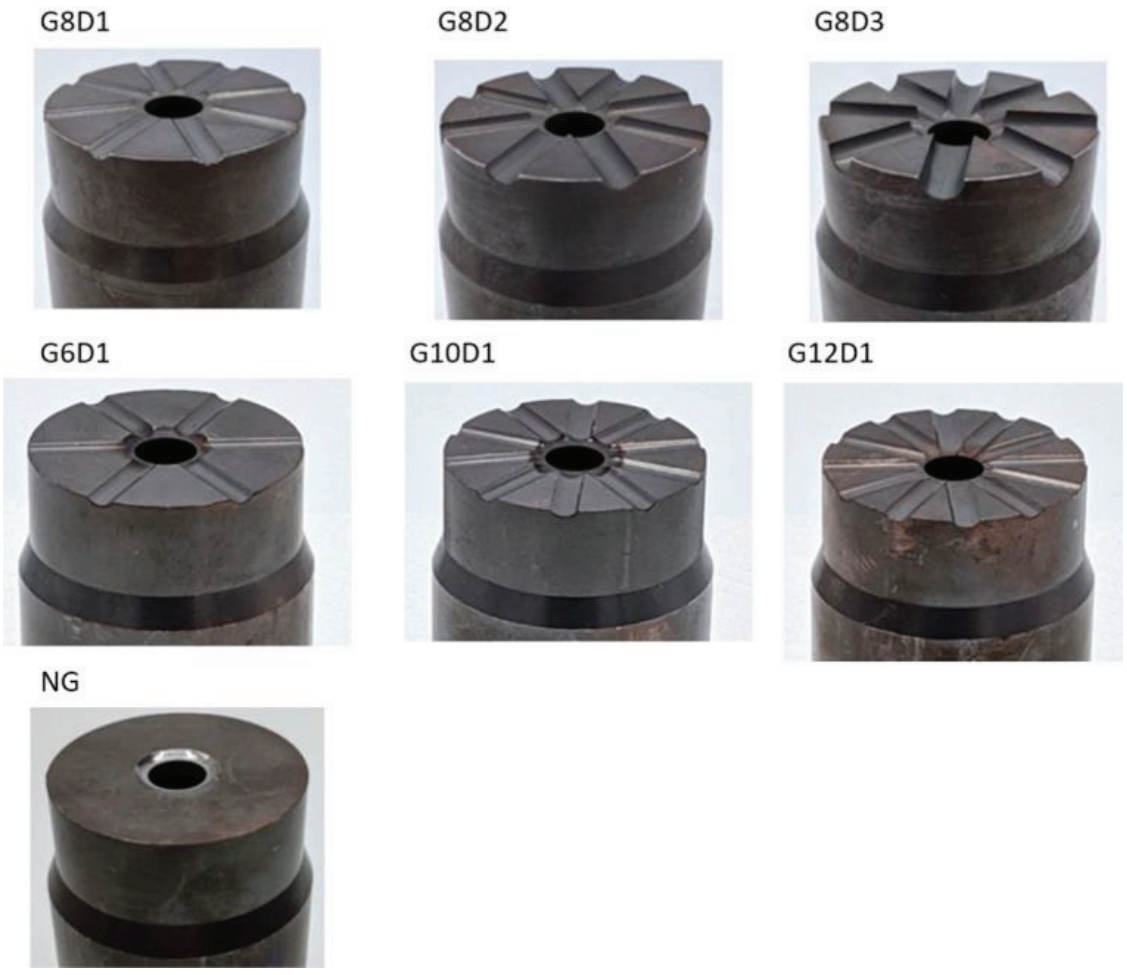

Fig. 6. Dies used for experimental research

properties comparable to those of the extrudate produced by dies with grooves. However, there is a noticeable decreasing trend with the sample location along the length of the extrudate. The value of the yield strength decreases noticeably with the length of the extrudate.

The hot extrusion test using the conventional process produced extrudate with noticeably lower tensile strength and relative elongation.

In both cases, the elongation values marked in red in Table 5 are the result of specimens breaking outside the measurement area during the test.

The macrostructure of the alloys was evaluated on the samples made in cross sections. Observations of the samples in the undigested state did not reveal the presence of any defects formed during the extrusion process. The etching process revealed visible flow lines forming bands arranged circumferentially in the near-surface areas of all tested samples, regardless of the extrusion stage. Their density varies depending on the examined variant, reaching a maximum depth of about 0.5 mm (with a predominant depth of 0.2 to 0.4 mm) (Fig. 11).

For test NG, conventional hot extrusion, the presence of distinct peripheral flow lines was not observed after any of the deformation stages. Only after the initial stage (F), at a distance of about 0.8÷1.0 mm from the surface, a slight disruption of the microstructure is observed, arranged in the form of a ring about 0.2 mm wide (Fig. 12).

Observations of the microstructure of the specimens representing each sample and extrusion stage (F, M, E) included the near-surface area, where flow lines (high strain) were found, and the area

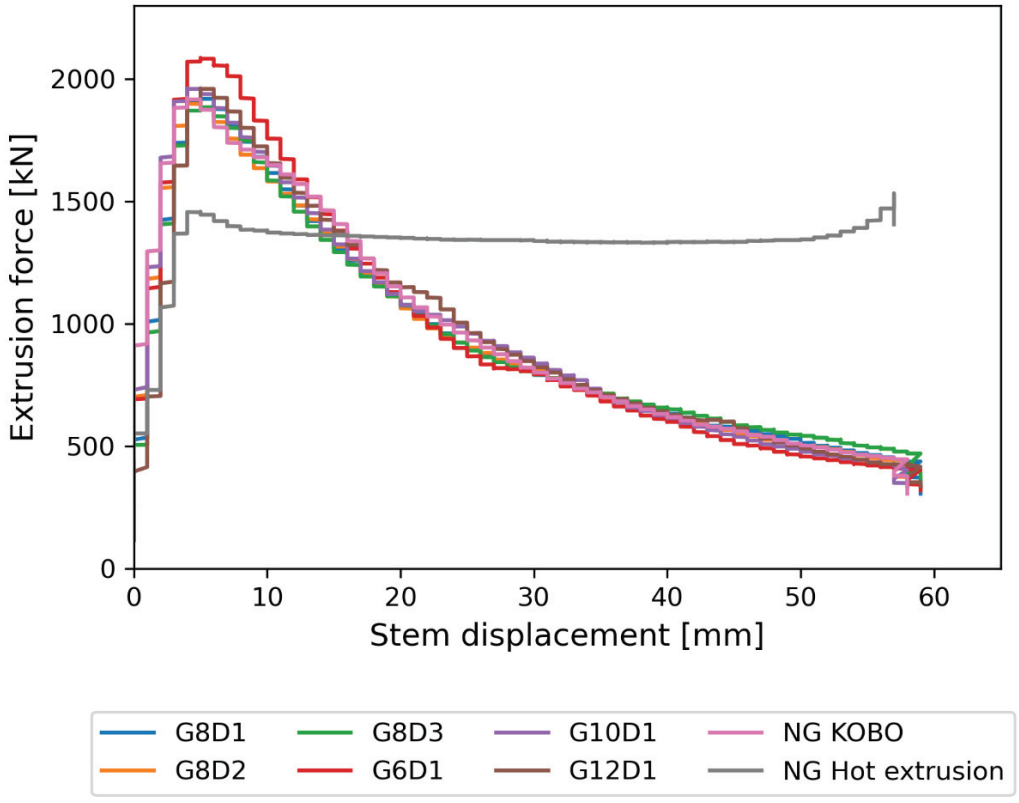

Fig. 7. Graph of the extrusion force as a function of stem displacement

Table 2. Maximum recorded extrusion forces in the KOBO process using different die types

Test	Maximum extrusion force [kN]	Comment
G8D1	2086	No container sleeve cleaning before test
G8D2	1962	
G8D3	1962	
G6D1	1924	
G10D1	1906	
G12D1	1890	
NG KOBO	1923	Flat face die
NG	1458	Conventional extrusion at 450°C
Butt	79	Butt pushing force while cleaning container sleeve

Table 3. Mechanical properties of extrudate determined by static tensile test – series 1

	$R_{p0.2}$	R_m	A_{50}
	MPa	MPa	%
G8D1F	194.3767	319.763	16.82835
G8D1M	182.0377	325.0069	15.53416
G8D1E	191.4832	351.6311	17.21147
G8D2F	191.682	329.3694	16.09939
G8D2M	184.0032	325.3811	17.21048
G8D2E	174.6589	327.0506	14.48359
G8D3F	191.8396	326.371	18.55923
G8D3M	179.7999	322.9885	17.81401
G8D3E	187.1591	344.8309	14.46475

in the rod axis. The microstructure of the 7075 alloy for all test specimens observed in the cross-section is characterized by fine, equiaxial grain sizes not exceeding 5 μm. There was no significant difference in grain size either by sample or by extrusion stage (F, M, E).

The microstructure of the alloy in the near-surface area for all examined samples (Fig. 13) is closely correlated with the macrostructure. The morphology of the particle precipitates of the

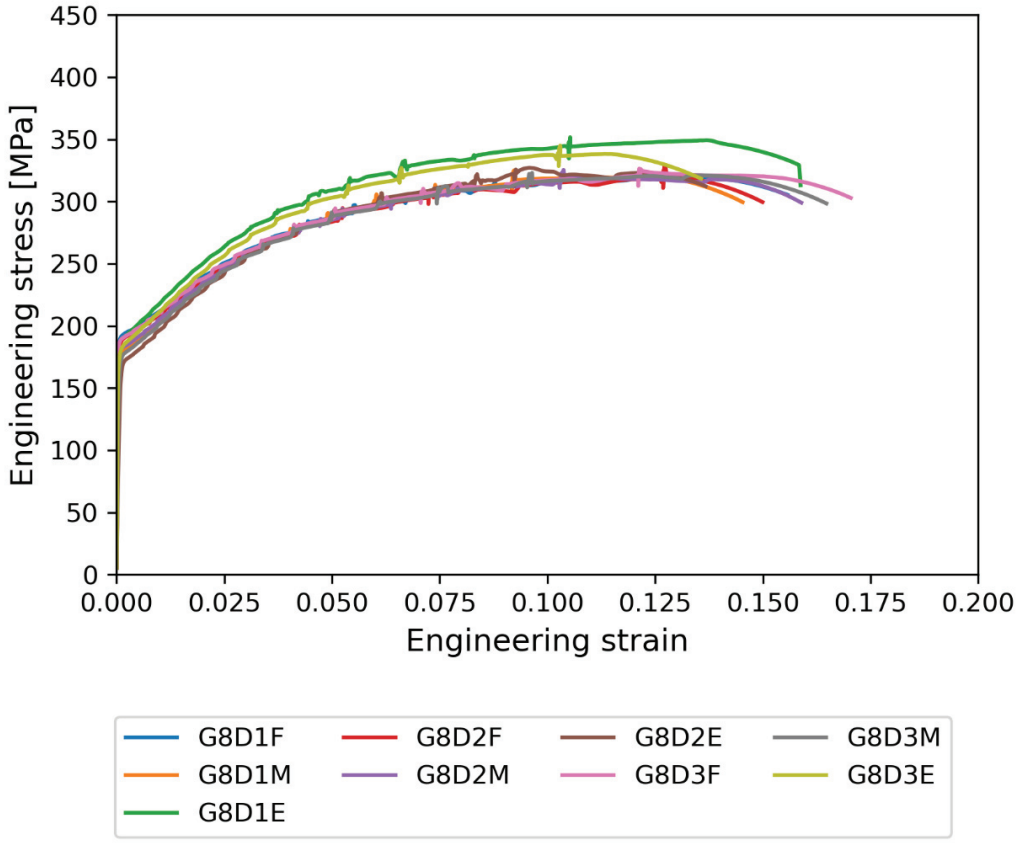

Fig. 8. Graph of stress-strain relationships in static tensile test of extruded products – samples taken from three areas along the length of the extrudate – series 1

Table 4. Mechanical properties of extrudate determined by static tensile test – series 2

	$R_{p0.2}$	R_m	A_{50}
	MPa	**MPa**	%
G6D1F	139.9892	375.7772	18.3135
G6D1M	203.2703	351.6911	15.75259
G6D1E	203.6512	357.1238	15.73096
G10D1F	219.1892	359.8165	17.40554
G10D1M	213.132	362.4292	17.7133
G10D1E	211.7307	372.7265	15.55199
G12D1F	228.0526	372.5014	16.29631
G12D1M	204.0853	361.9522	17.48726
G12D1E	217.7237	377.1663	13.81927

Table 5. Mechanical properties of extrudate determined by static tensile test – series 3

	$R_{p0.2}$	R_m	A_{50}
NG_KOBO F	227.5532	363.6127	11.61306
NG_KOBO M	210.6277	368.3837	37.3797
NG_KOBO E	194.2238	354.8399	16.83634
NG F	178.6093	314.8302	12.87594
NG M	178.4273	318.8969	27.68791
NG E	179.8115	303.1239	9.513819

intermetallic phases corresponds to the course and arrangement of the flow lines. In the area of lower density of the lines, we observed an almost complete absence of particles of the strengthening phase $MgZn_2$, appearing in the form of large, dark precipitates, and a much smaller amount of the other intermetallic phases visible in the form of very fine, bright precipitates. In the areas of higher concentration of the flow lines, there is a greater number of intermetallic phases. Outside the area where the bands/flux lines are present, the particle distribution of the separated intermetallic phases is uniform.

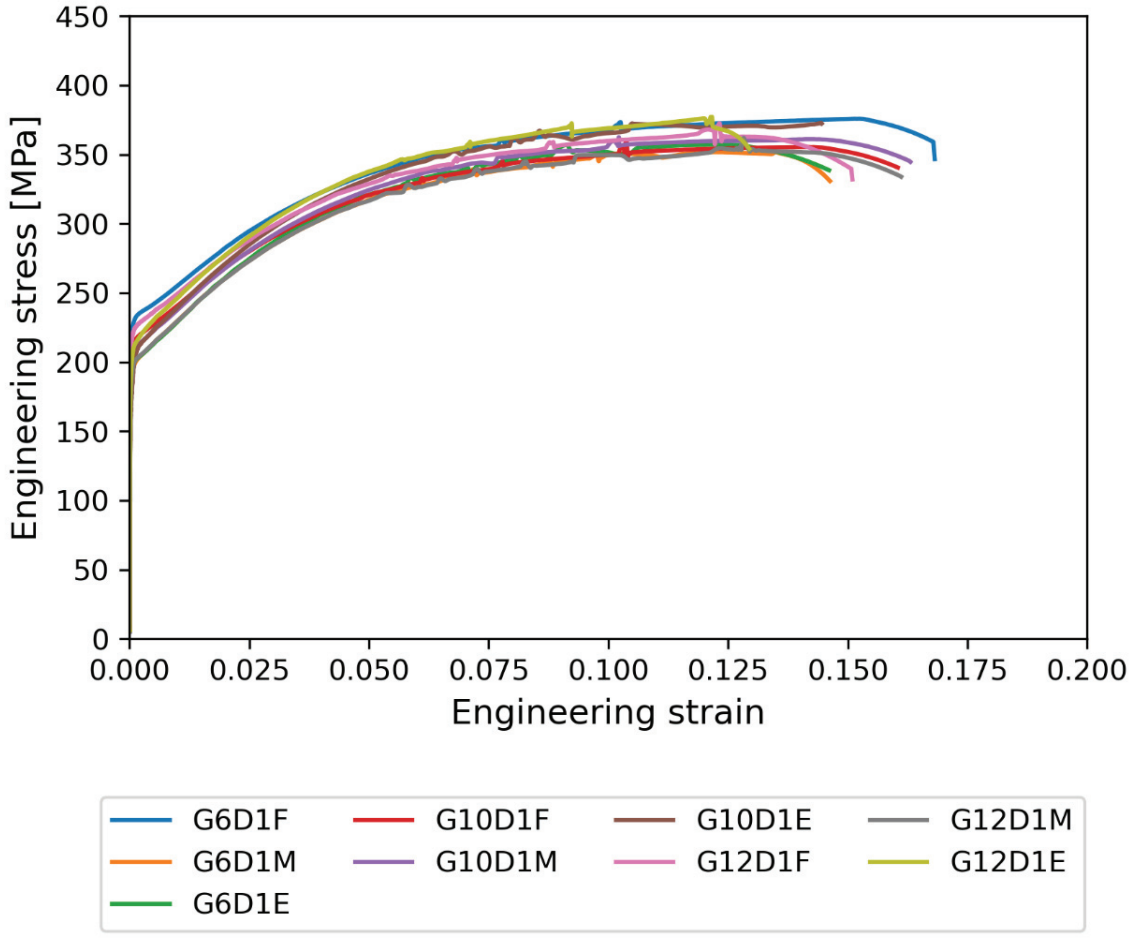

Fig. 9. Graph of stress-strain relationships in static tensile test of extruded products – samples taken from three areas along the length of the extrudate – series 2

However, between the initial state and after the extrusion process, the number and size of the $MgZn_2$ phase precipitates in the microstructure of the alloy decreased (fig. 14). A tendency for these parameters to decrease depending on the stage of extrusion was also observed, according to the F>M>E relationship.

The microstructure of the NG test (conventional hot extrusion) samples after deformation (Fig. 15) is the same for all stages of deformation (F, M, E). However, discrepancies were observed in its structure compared to the "typical" microstructure characteristic of alloy 7075 after the KOBO deformation process, which was observed for the variants examined earlier. Although the phase composition of the alloy did not change, differences were found in the morphology of the phase components. Observations using light optical microscopy showed variations in the relative volume and particle size of the Al_2CuMg strengthening phase, which could be observed on both the cross-sectional and longitudinal sections of the rods. Separations of the strengthening phase are finer and there are significantly fewer of them compared to other deformation variants. The use of a scanning electron microscope (SEM) magnifying up to 3000x (Fig. 16) revealed the presence of dispersed superfine particles of the strengthening intermetallic phases $MgZn_2$ and Mg(Zn, Al, Cu), which have been partially or completely spheroidized. Their relative volume also increased compared to the alloy after the KOBO deformation

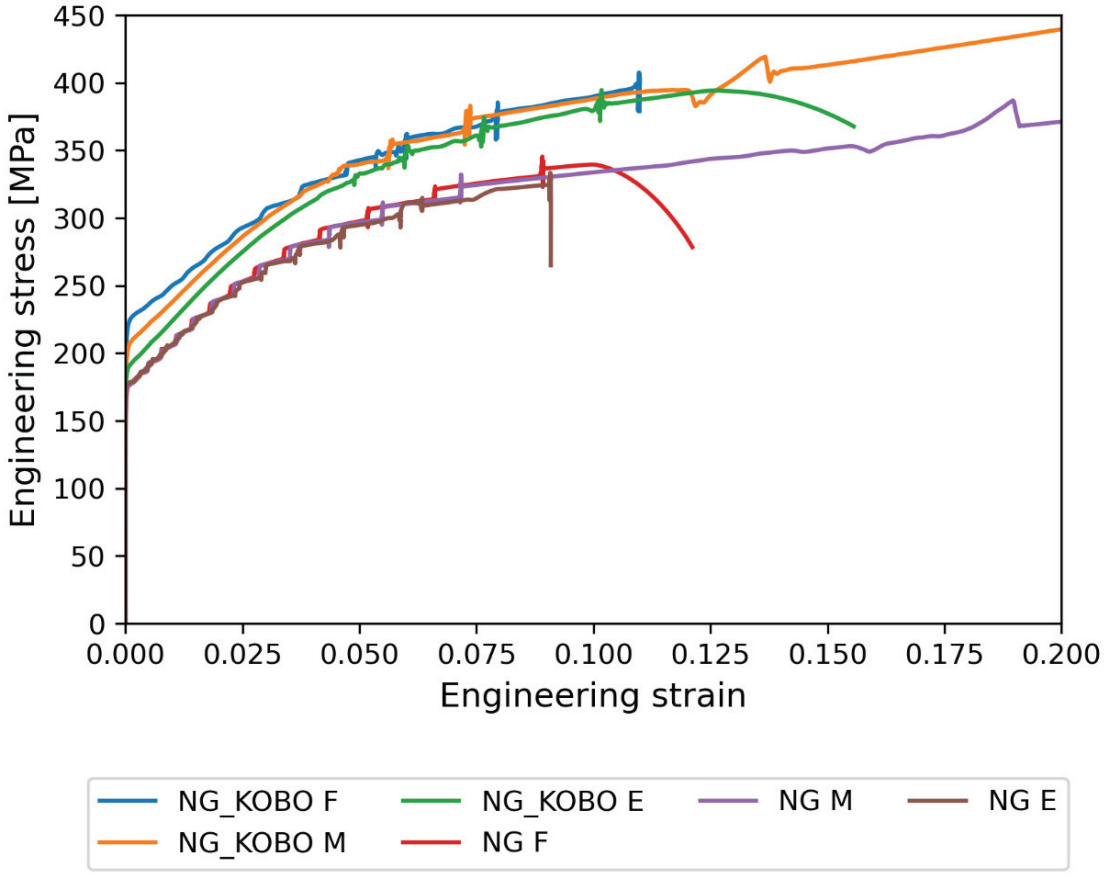

Fig. 10. Graph of stress-strain relationships in static tensile test of extruded products – samples taken from three areas along the length of the extrudate – series 3

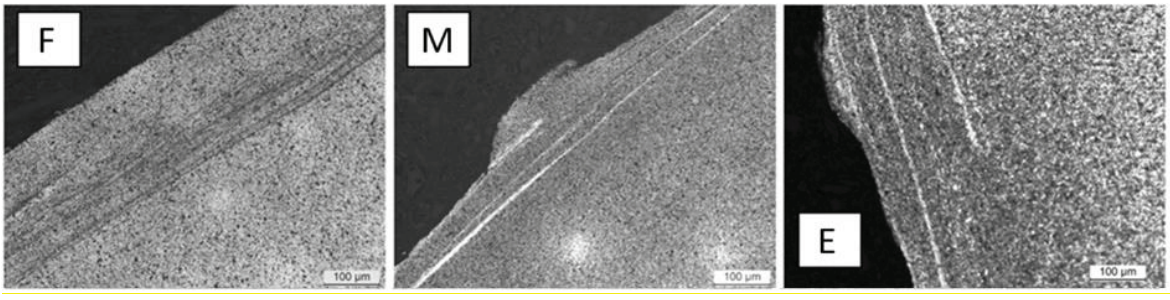

Fig. 11. Macrostructure of 7075 alloy: front, 200x mag.; middle, 100x mag.; and end extrusion stages, 100x mag. Visible shear lines in the near-surface area

process. Such changes in microstructure are characteristic of the alloy's aging process, which occurs under the influence of temperatures higher than the aging temperature.

In the case of the microstructure of samples from test NG, significant inhomogeneity of the morphology of the phase components is apparent, related to the banding typical of conventionally extruded bars.

The mechanical properties of the samples from the obtained extrudate show similar properties for all samples within a given series, which shows that

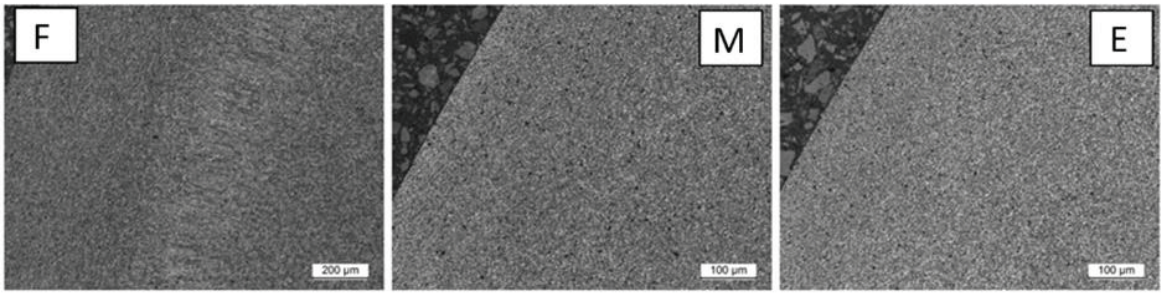

Fig. 12. Macrostructure of alloy 7075 after conventional extrusion: front, middle and end extrusion stages, 100x mag. No clear shear lines, visible peripheral disruption of the alloy microstructure due to flow

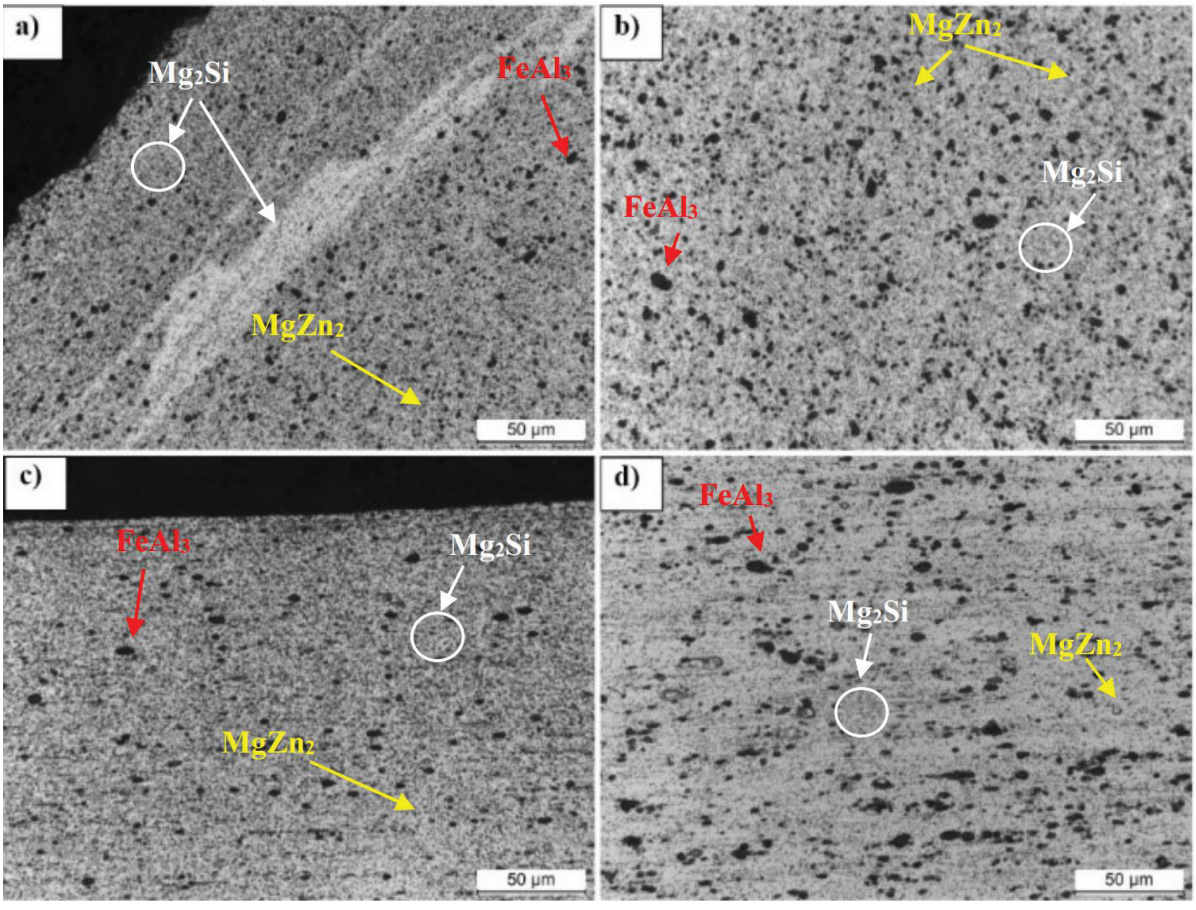

Fig. 13. Microstructure of 7075 alloy: cross-sectional view of the near-surface area (a) and the area inside the bar (b), and longitudinal section of the near-surface area (c) and the area inside the bar (d), 500x mag

the use of grooves with different geometries on the die faces does not significantly affect the tensile properties of the obtained extrudate. Extruded samples obtained using a die with a flat face in the KOBO process show a decrease in mechanical properties, especially the yield strength with the location of the sample. These results indicate that in this case the implementation of the process generates higher heats that decrease the properties of the pressboard, higher than in the initial phase of the process with a downward trend. The strength properties of the extruded samples obtained in

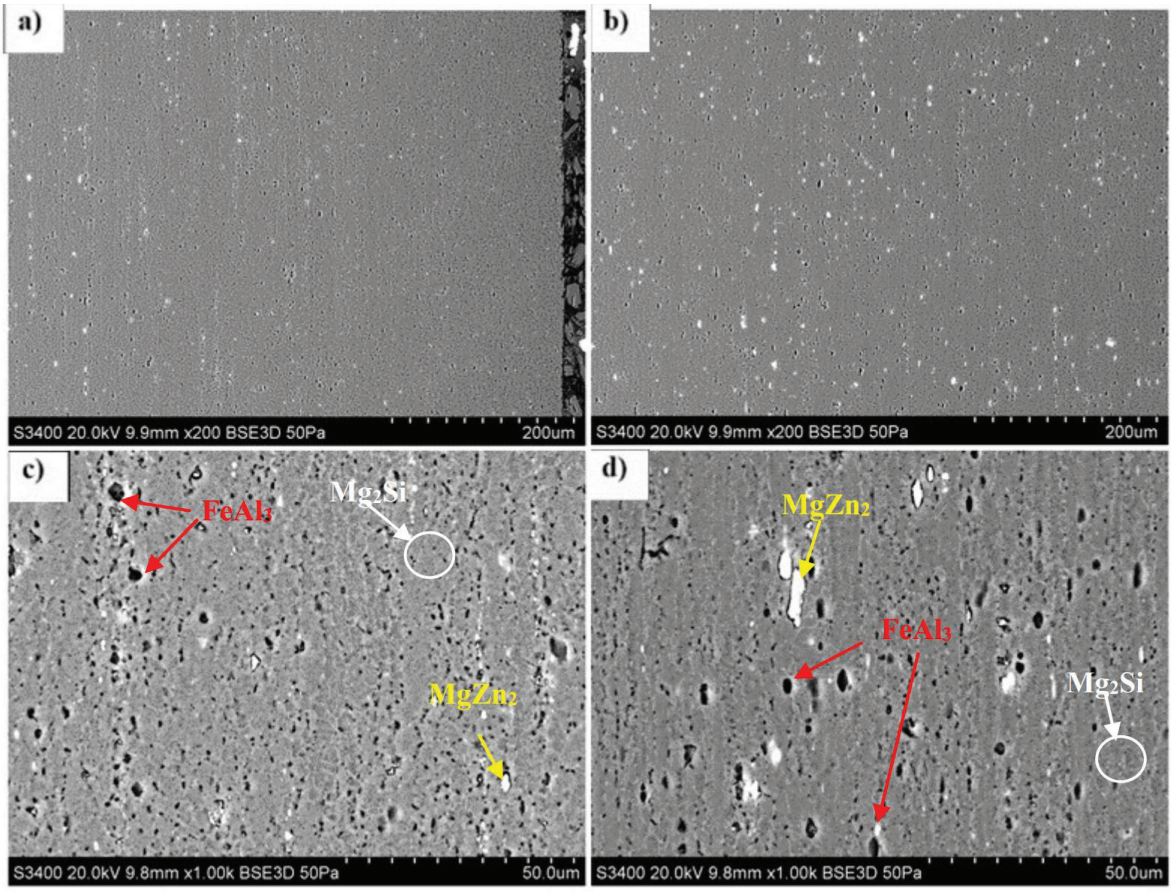

Fig. 14. Microstructure of 7075 alloy typical of all tested KOBO samples in the near-surface zone (a and c, 200x mag.) and beyond (b and d, 1000x mag.). Longitudinal section, SEM

the conventional hot extrusion test are lower than for the rest of the samples obtained from the KOBO process, which was predictable due to the realization of the process at a temperature above the recrystallization temperature of the extruded material.

All of the samples of extrudate produced by dies with face grooves show analogous internal macro and microstructure and morphology. The internal structure of the specimens correlates with the results obtained from testing the strength properties of the extruded product. The use of annealed material for testing and the analysis of the test results allow us to conclude that the input material, aluminum alloy 7075 subjected to precipitation strengthening, was strengthened only by plastic deformation. This fact indicates that the temperature emitted during the process is lower ($<\sim$470°C) and its influence is too short to activate the supersaturation process, and the material after extrusion did not undergo natural aging until the realization of strength tests. On all specimens obtained from the pressboard after the KOBO process, there is a clearly visible encirclement of the outer area of the expression bars that differs in structure from the structure closer to the axis of the extruded rod. This zone reaches a thickness of $\sim$0.2–0.5 mm and, in relation to the structure of the material in the rest of the product volume, does not show clear features of deformation in the axial direction band structure. In the near-surface areas of the extrudate, a higher concentration of fragmented intermetallic phases was found. This gives rise to the conclusion that the material in the near-surface zone comes from an area of the billet that has been subjected to more intense

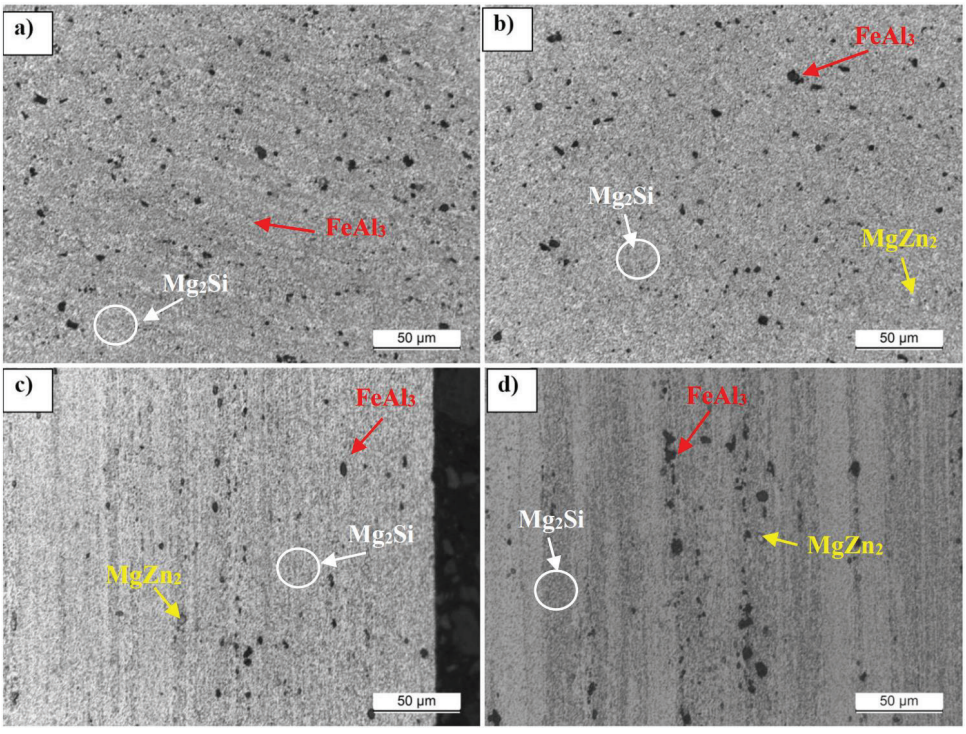

Fig. 15. Microstructure of 7075 alloy, test NG (F): cross-section of the near-surface area (a) and the area inside the bar (b) and longitudinal cross-section of the near-surface area (c) and the area inside the bar (d), 500x mag

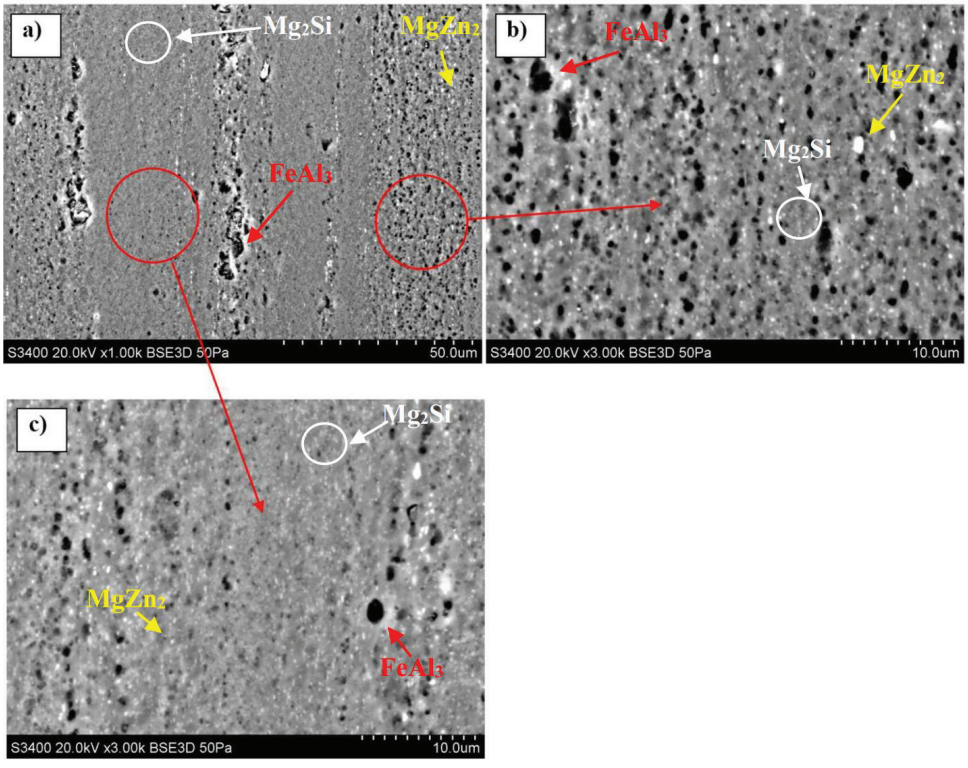

Fig. 16. Microstructure of the extrudate, sample NG (F): longitudinal cross-section, visible inhomogeneity due to the banded structure of the rod, SEM, (a) 1000x mag., (b) & (c) 3000x mag

plastic deformation. Regardless of the location of the sample from the pressboard (F, M, E) obtained by the KOBO method, the internal structure of the product is the same, showing no significant change in microstructure along the length of the product.

4. Conclusions

The KOBO method is an efficient method for extruding light metal alloys (in this case, aluminum alloy) in a process carried out without heating the billets and press components. The extrudate obtained during the experimental research is characterized by the same mechanical and structural properties regardless of the location of the test samples. The products obtained by the cold KOBO process do not bear the features of the influence of elevated temperature. The use of dies with different geometries of the front part reduced the extrusion force. The lowest extrusion force registered was 1890 kN, compared to >1900 kN in other performed tests. This indicates that the modification of the die face has a direct effect on the formation of a zone of intense plastic deformation near the die face, and conventional cold extrusion in the examined case is impossible to perform. Attention should be paid to the effects of microstructure transformation shown in this paper, specific for "cold" extrusion of KOBO, in comparison to the data presented in numerous publications on alloy 7075 extruded by traditional “hot” processes [18–20]. Extrusion by the KOBO method using a flat die was feasible; however, the extrudate bears signs of increased heat generation during the process, most likely due to friction. Circumferential shear bands in the near-surface zone of the extrudate, occurring in all analyzed samples obtained by the KOBO method, with an internal structure different from that observed near the axis of the rods, indicate that this is a volume of material that comes from the zone of intense plastic deformation. The volume of material closer to the bar axis shows features corresponding to axial plastic flow, which indicates that the billet material is deformed by moving along the zone of intense plastic deformation without being subjected to deformation in complex strain conditions.

References

[1] Korbel A, Bochniak W. *Method of plastic forming of materials*. US5737959A, 1998 [Accessed 8th August 2020]. https://patents.google.com/patent/US5737959/en?oq=korbel+bochniak [Accessed 8th August 2020].

[2] Bochniak W, Korbel A. *Method of plastic forming of materials*. EP0711210B1, 2000 [Accessed 8th August 2020]. https://patents.google.com/patent/EP0711210B1/en?oq=korbel+bochniak [Accessed 8th August 2020].

[3] Bochniak W. *Teoretyczne i praktyczne aspekty plastycznego kształowania metali: metoda KoBo*. Kraków: Wydawnictwa AGH; 2009.

[4] Sztwiertnia K, Kawałko J, Bieda M, Berent K. Microstructure of Polycrystalline Zinc Subjected to Plastic Deformation by Complex Loading / Mikrostruktura Polikrystalicznego Cynku Odkształconego Plastycznie W Złozonym Schemacie Deformacji. *Arch. Metall. Mater*. 2013;58(1): 157–161. doi: 10.2478/v10172-012-0167-4

[5] Bochniak W, Korbel A, Ostachowski P, Ziółkiewicz S, Borowski J. Wyciskanie metali i stopów metodą KOBO. *Obróbka Plastyczna Metali*. 2013;XXIV(2).

[6] Korbel A, Bochniak W, Ostachowski P, Błaż L. Visco-Plastic Flow of Metal in Dynamic Conditions of Complex Strain Scheme. *Metall. Mater. Trans. A*. 2011;42(9): 2881–2897. doi: 10.1007/s11661-011-0688-x

[7] Zwolak M, Śliwa RE. Fizyczne modelowanie plastycznego płyniêcia w procesie wyciskania metodą KOBO z użyciem matryc o różnej geometrii. *Obróbka Plastyczna Metali*. 2017;28(4). http://yadda.icm.edu.pl/baztech/element/bwmeta1.element.baztech-03be5e17-d90d-4187-8020-9f026b33aed2

[8] Korbel A, Bochniak W. Refinement and control of the metal structure elements by plastic deformation. *Scr. Mater*. 2004;51(8): 755–759. doi: 10.1016/j.scriptamat.2004.06.020

[9] Korbel A, Pieła K, Ostachowski P, Łagoda M, Błaż L, Bochniak W, et al. Structural phenomena induced in the course of and post low-temperature KOBO extrusion of AA6013 aluminum alloy. *Mater. Sci. Eng., A*. 2018;710: 349–358. doi: 10.1016/j.msea.2017.10.095

[10] Balawender T, Zwolak M, Bąk Ł. Experimental Analysis of Mechanical Characteristics of KOBO Extrusion Method. *Arch. Metall. Mater*. 2020;65(2): 615–619. doi: 10.24425/AMM.2020.132800.

[11] Kong LX, Hodgson PD, Wang B. Development of constitutive models for metal forming with cyclic strain softening. *J. Mater. Process. Technol*. 1999;89–90: 44–50. doi: 10.1016/S0924-0136(99)00015-1

[12] Kong LX, Hodgson PD. Constitutive modelling of extrusion of lead with cyclic torsion. *Mater. Sci. Eng., A*. 2000;276(1–2): 32–38. doi: 10.1016/S0921-5093(99)00511-0.

[13] Maciejewski J, Mróz Z. An upper-bound analysis of axisymmetric extrusion assisted by cyclic torsion.

J. Mater. Process. Technol. 2008;206(1–3): 333–344. doi: 10.1016/j.jmatprotec.2007.12.061.

[14] Lukaszkowicz K. Forming the structure and properties of hybrid coatings on reversible rotating extrusion dies. *J. Achiev. Mater. Manuf. Eng*. 2012;55(2): 66.

[15] Wójcik M, Skrzat A. The Coupled Eulerian-Lagrangian Analysis of the KOBO Extrusion Process. *Adv. Sci. Technol. Res. J.* 2021;15(1): 197–208. doi: 10.12913/22998624/131663.

[16] Totten GE, Tiryakioğlu M, Kessler O, [eds.]. *Encyclopedia of Aluminum and Its Alloys, Two-Volume Set (Ebook)*. 1st ed. Boca Raton, FL: CRC Press; 2018.

[17] J. R. Davis & Associates, ASM International, [eds.]. *Aluminum and aluminum alloys*. Materials Park, OH: ASM International; 1993.

[18] Sheppard T, Tunnicliffe PJ, Patterson SJ. Direct and indirect extrusion of a high strength aerospace alloy (AA 7075). *J. Mech. Work. Technol*. 1982;6(4): 313–331. doi: 10.1016/0378-3804(82)90031-6.

[19] Rokni MR, Zarei-Hanzaki A, Abedi HR, Haghdadi N. Microstructure evolution and mechanical properties of backward thixoextruded 7075 aluminum alloy. *Mater. Des*. 2012;36: 557–563. doi: 10.1016/j.matdes.2011.11.061.

[20] Song Y, Zhang Z, Wang K, Li H, Zhu Z. Effects of Extrusion Processing on Microstructure of 7075Al Alloy in the Semi-solid State. *J. Wuhan Univ. Technol. Mater. Sci. Ed.* 2019;34(6): 1433–1443. doi: 10.1007/s11595-019-2210-z.

Received 2023-12-29
Accepted 2024-04-24